Energy dependence of (p,t) analyzing powers arising from strong, sequential, two-step processes with j dependence

K. Yagi, H. Iida,* Y. Aoki, K. Hashimoto, and Y. Tagishi
Institute of Physics and Tandem Accelerator Center, University of Tsukuba, Ibaraki 305, Japan
(Received 4 September 1984)

A marked variation of the analyzing power $A(\theta)$ with incident proton energy for the ground-state ($0^+_{g.s.}$) transition of ^{92}Zr(p,t)^{90}Zr($0^+_{g.s.}$) was observed over a proton-energy range from 17.0 to 28.5 MeV in the angular region around $\theta \approx 20°$ where the corresponding (p,t) cross section $\sigma(\theta)$ yields the first minimum. On the other hand, no such an energy variation was observed at all in the analyzing power for the ground-state transition of ^{138}Ba(p,t)^{136}Ba($0^+_{g.s.}$) over the same energy range. The former analyzing power shows an "anomalous" angular distribution which deviates essentially from the derivative rule $\{A(\theta)=[d\sigma(\theta)/d\theta]/\sigma(\theta)\}$, while the latter analyzing power shows a "normal" angular distribution. In contrast to the analyzing-power angular distributions, the cross-section angular distributions of the two reactions are quite similar and do not show any remarkable energy variation. All these characteristic features of the two reactions are explained by taking account of strong, sequential (p,d)(d,t) two-step processes in addition to a (p,t) one-step process in terms of the first- and second-order distorted-wave Born approximation. The nuclear-shell orbit dependence (j dependence) of the analyzing powers for the (p,d)(d,t) two-step process plays an essential role in producing the distinguished difference in the energy dependence of the observed analyzing powers for the two reactions. When two neutrons are picked up sequentially from a $j_> = l + \frac{1}{2}$ ($j_< = l - \frac{1}{2}$) orbit, such as a $d_{5/2}$ ($d_{3/2}$) orbit in the case of the ^{92}Zr(p,t)^{90}Zr [^{138}Ba(p,t)^{136}Ba] reaction, the two-step analyzing power is quite different from (similar to) the one-step analyzing power so that the total analyzing power shows a completely different (similar) angular distribution from (to) the one-step analyzing power in the forward angles. The interference effect between the one- and two-step processes is thus quite sensitive to (quite stable against) the relative phase between the transition amplitudes of the two processes. Therefore ^{92}Zr(p,t) [^{138}Ba(p,t)] analyzing power shows a marked (no marked) change with incident energy. The nuclear structure involved in the reaction ^{138}Ba(p,t)^{136}Ba is calculated on the basis of the monopole-pairing vibrational model. The cross section of the (p,d)(d,t) two-step processes is as large as that of the one-step process, so that the resultant total cross section obtained from the coherent sum of the two processes can reproduce the absolute magnitude of the experimental cross sections for the $0^+_{g.s.} \rightarrow 0^+_{g.s.}$(p,t) reactions well. The derivative rule for $0^+_{g.s.} \rightarrow 0^+_{g.s.}$(p,t) reactions is derived within the framework of the first-order distorted-wave Born approximation.

I. INTRODUCTION

After introducing a completely new type of experimental probe, the understanding of a phenomenon which has been assumed to be already complete can sometimes turn out to be by no means complete and even short of essential points. Contrary to differential cross sections $\sigma(\theta)$ for reactions with unpolarized beams, analyzing powers $A(\theta)$ for reactions with polarized beams can be regarded as such a probe. Realizing that analyzing powers $A(\theta)$ are much more sensitive to interferences between various competing reaction processes than the corresponding cross sections $\sigma(\theta)$ (Ref. 1), we have extensively utilized analyzing powers as a powerful probe not only for the investigation of reaction mechanisms[1–11] but also for the study of microscopic structures of nuclei[12–18] and of effective nuclear forces.[19,20]

It should be emphasized that because of the high sensitivity to interference effects between various nuclear transition amplitudes, analyzing power measurements are quite useful for solving problems which are not related directly to a spin-dependent interaction. Actually, "anomalous" analyzing powers for strong (p,t) ground state $0^+(0^+_{g.s.})$ to $0^+_{g.s.}$ transitions, which have been first observed by the Tsukuba group[2] using a 22-MeV polarized proton beam, provide direct experimental evidence for strong, sequential, two-step (p,d)(d,t) transfer processes in *allowed* (p,t) reactions. In addition, an analyzing power measurement of an almost *"forbidden"* unnatural-parity transition ^{208}Pb(p,t)^{206}Pb(3^+,1.34 MeV), which has been carried out also by the Tsukuba group,[3] provides a definite conclusion on its reaction mechanism: the predominance of the (p,d)(d,t) two-step mechanism over the one-step (p,t) mechanism.[7,21]

The above-mentioned (p,t) analyzing powers for the $0^+_{g.s.} \rightarrow 0^+_{g.s.}$ transitions have been found to exhibit a marked nuclear shell effect which results from their (p,d)(d,t) two-step processes.[1,16] Indeed, the observed analyzing powers can be classified into two types with respect to whether the picked-up neutrons belong to a nuclear shell of $j_> = l + \frac{1}{2}$ or $j_< = l - \frac{1}{2}$ (Ref. 16). In the first case of the $j = j_>$ shell an anomalous (p,t) analyzing

power which does not satisfy a derivative relation ($A(\theta) \simeq [d\sigma(\theta)/d\theta]/\sigma(\theta)$) appears, while in the second case of the $j = j_<$ shell no such anomalous analyzing powers appear.

In the present paper we investigate the energy dependence of the (p,t) analyzing powers on the basis of the above-mentioned nuclear shell effect which arises from the two-step processes. Actually we measured the analyzing powers and cross sections for the $0^+_{g.s.} \rightarrow 0^+_{g.s.}$ transitions of ^{92}Zr(p,t)^{90}Zr and ^{138}Ba(p,t)^{136}Ba over a wide region of incident proton energy from 17 to 29 MeV. The reason why we chose these two targets is the following: In the ^{92}Zr(p,t)^{90}Zr($0^+_{g.s.}$) transition of $N = 52 \rightarrow 50$, the picked-up neutrons belong mainly to the $j_> = d_{5/2}$ shell, while in the ^{138}Ba(p,t)^{136}Ba($0^+_{g.s.}$) transition of $N = 82 \rightarrow 80$, the neutrons belong mainly to the $j_< = d_{3/2}$ shell. A preliminary report on the reaction ^{92}Zr(p,t)^{90}Zr($0^+_{g.s.}$) [^{138}Ba(p,t)^{136}Ba($0^+_{g.s.}$)] for $E_p = 20$–22.5 (18.5–21.0) MeV was given in Ref. 4 (5).

II. EXPERIMENT AND RESULTS

The experiment with polarized proton beams of energies from $E_p = 17.0$ to 22.5 MeV was made at the Tandem Accelerator Center, University of Tsukuba by using the UTTAC 12 UD Pelletron, while the one at $E_p = 28.5$ MeV was carried out at the Institute for Nuclear Study (INS), University of Tokyo by using the Sector Focusing Cyclotron.

The polarized proton beam at UTTAC was produced with a Lamb-shift–type polarized ion source.[22] The typical beam intensity on the target and the beam polarization was 100 nA and (80±1) %, respectively. Emitted charged particles were analyzed with a magnetic spectrograph[23] and were detected with a single-wire proportional counter (SWPC).[24] The experimental procedure was the same as that of the previous papers,[3,8] thus no detailed description about it is given here. We measured vector analyzing powers $A(\theta)$ and differential cross sections $\sigma(\theta)$ from $\theta_{lab} = 5°$ to 65° in 5° or 2.5° steps with an angular acceptance of the magnetic spectrograph $\Delta\theta_{lab} = 1.5°$ or 3.0°, except for the case of the reaction ^{92}Zr(p,t)^{90}Zr at $E_p = 22.0$ MeV, where the measurement was made from $\theta_{lab} = 5°$ to 115°.

The polarized proton beam of $E_p = 28.5$ MeV at INS was produced with an atomic-type polarized ion source. The typical beam intensity on target and the beam polarization was 10 nA and (40±3) %, respectively. A ^{12}C polarimeter (the analyzing power $A = 0.58$ at $\theta_{lab} = 62°$ for elastic scattering of 28.5-MeV protons) was placed upstream the scattering chamber. Emitted charged particles were analyzed with a QDD spectrograph[25] and were detected with a multiwire proportional counter system.[26] The analyzing powers and cross sections for the reactions ^{92}Zr(p,t)^{90}Zr and ^{138}Ba(p,t)^{136}Ba were measured from $\theta_{lab} = 5°$ to 55° in 2.5° steps with an angular spread of the spectrograph of $\Delta\theta_{lab} = 1.8°$.

We made the experiments on the reactions ^{92}Zr(p,t)^{90}Zr($0^+_{g.s.}$) and ^{138}Ba(p,t)^{136}Ba($0^+_{g.s.}$) by using the targets of which characteristics are given in Table I. The energy resolutions obtained were mainly due to the target thicknesses. Measured angular distributions of the analyzing powers $A(\theta)$ and the cross sections $\sigma(\theta)$ for the reactions are shown in Figs. 1 and 2. Error bars where uncertainties exceed the size of the circles, etc., indicate statistical and systematic uncertainties. In addition to these errors, the absolute values of the cross sections $\sigma(\theta)$ are estimated to have an error of 20%, which is mainly ascribed to an uncertainty in the target thickness.

The analyzing powers $A(\theta)$ and the cross sections $\sigma(\theta)$ for the reaction ^{92}Zr(p,t)^{90}Zr($0^+_{g.s.}$) [^{138}Ba(p,t)^{136}Ba($0^+_{g.s.}$)] were measured at $E_p = 17.0$, 18.5, 20.1, 21.0, 21.5, 22.0, 22.5, and 28.5 MeV (18.5, 20.2, 21.0, 22.0, and 28.5 MeV). Characteristic features of the observed analyzing powers and the cross sections are the following:

(i) The analyzing powers for the reaction ^{92}Zr(p,t)^{90}Zr show a drastic change with incident proton energy in the angular region around $\theta \approx 20°$ where the corresponding cross sections yield the first minimum.

(ii) The analyzing powers for ^{92}Zr(p,t)^{90}Zr around $\theta \approx 20°$ show anomalous analyzing powers which deviate markedly from the derivative rule $A(\theta) \simeq [d\sigma(\theta)/d\theta]/\sigma(\theta)$.

(iii) In contrast to characteristic (i), the analyzing powers for the reaction ^{138}Ba(p,t)^{136}Ba do not show any pronounced variation with incident proton energy even

TABLE I. Characteristics of targets used in the reactions ^{92}Zr(p,t)^{90}Zr($0^+_{g.s.}$) and ^{138}Ba(p,t)^{136}Ba($0^+_{g.s.}$).

Target	Target thickness (mg/cm^2)	Chemical form	Isotopic purity (%)	Energy resolution (keV)	g.s. Q value[a] (MeV)
^{92}Zr	1.97[d,e]	Zr[b]	95.1	50[d,e]	−7.353
^{138}Ba	1.50[d]	$BaCO_3$[c]	99.7	60[d]	−7.035
^{138}Ba	2.82[e]	$BaCO_3$[c]	99.7	100[e]	

[a]Reference 37.
[b]Self-supporting metallic foil.
[c]Centrifugal settling method and on an aluminum backing of 7 μm thickness.
[d]For the $E_p \leq 22$ MeV experiment.
[e]For the $E_p = 28.5$ MeV experiment.

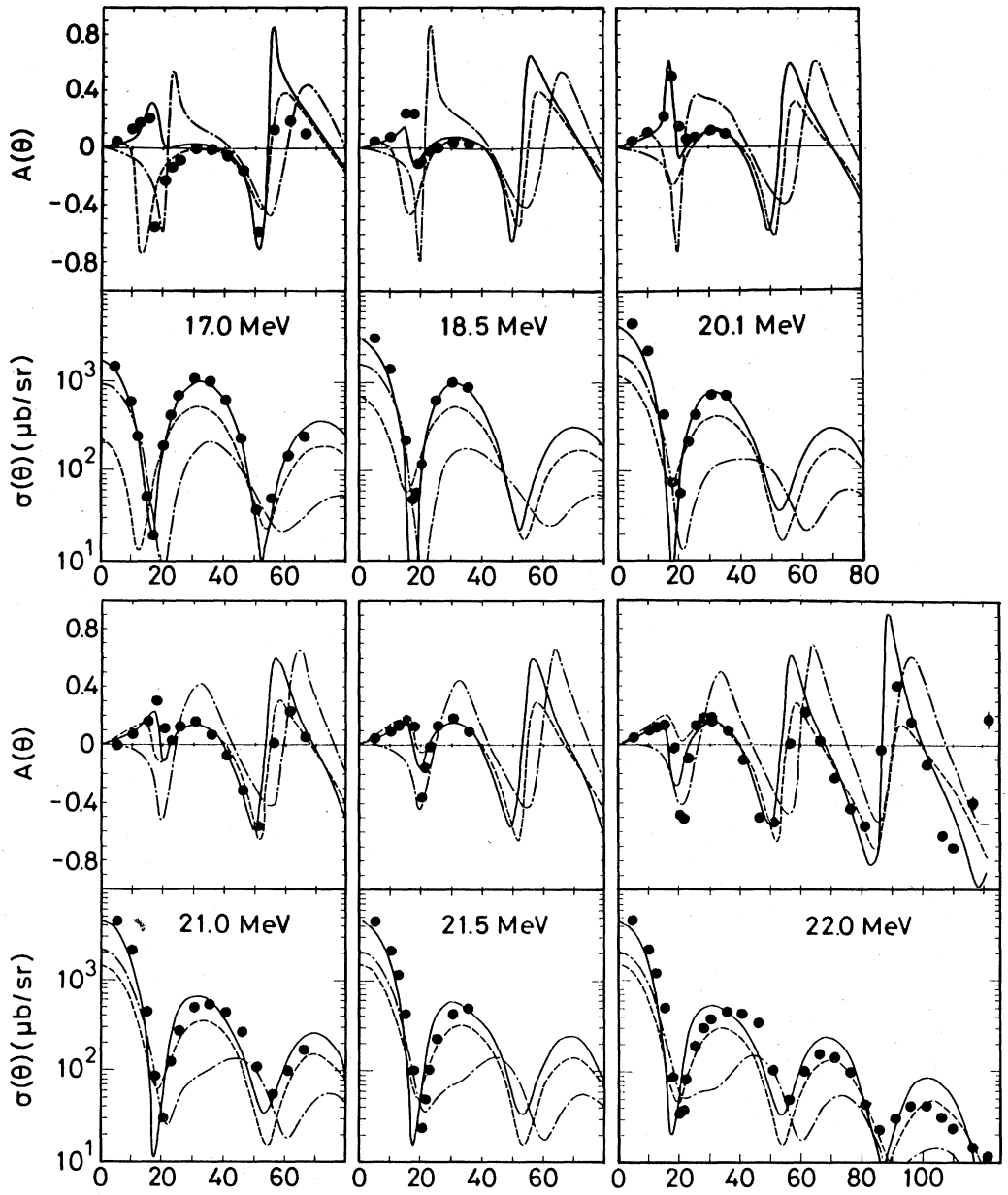

FIG. 1. Experimental and calculated analyzing powers $A(\theta)$ and cross sections $\sigma(\theta)$ for the reaction ^{92}Zr(p,t)^{90}Zr($0^+_{g.s.}$) at eight proton energies in the laboratory system. Dash-dotted (dashed) curves are the first-order [(p,d) (d,t) second-order] DWBA calculations and solid curves are the coherent sum of the two processes.

around $\theta \approx 15°$ where the corresponding cross sections give the first minimum.

(iv) In contrast to characteristic (ii), the analyzing powers for ^{138}Ba(p,t)^{136}Ba around $\theta \approx 15°$ do not show any anomalous analyzing powers.

(v) In contrast to the above-mentioned distinguished difference between the analyzing powers for the two reactions ^{92}Zr(p,t)^{90}Zr and ^{138}Ba(p,t)^{136}Ba, the cross sections for the two reactions show quite similar oscillation patterns with each other in angular distributions. Both cross sections do not exhibit any marked change with incident proton energy in their angular distributions.

TABLE II. Two-neutron separation energy S(2n), one-neutron separation energy S(n), reaction Q values for the reactions (p,t), (p,d), and (d,t). All are in units of MeV (Ref. 37). $S(2n) = -Q(p,t) + 8.482$, $S(n) = -Q(p,d) + 2.225$, and $S(n) = -Q(d,t) + 6.258$.

Target	^{92}Zr	^{91}Zr(g.s.)	^{138}Ba	^{137}Ba(g.s.)
S(2n)	15.835		15.517	
S(n)	8.641	7.195	8.611	6.907
Q(p,t)	−7.353		−7.035	
Q(p,d)	−6.416		−6.386	
Q(d,t)		−0.937		−0.649

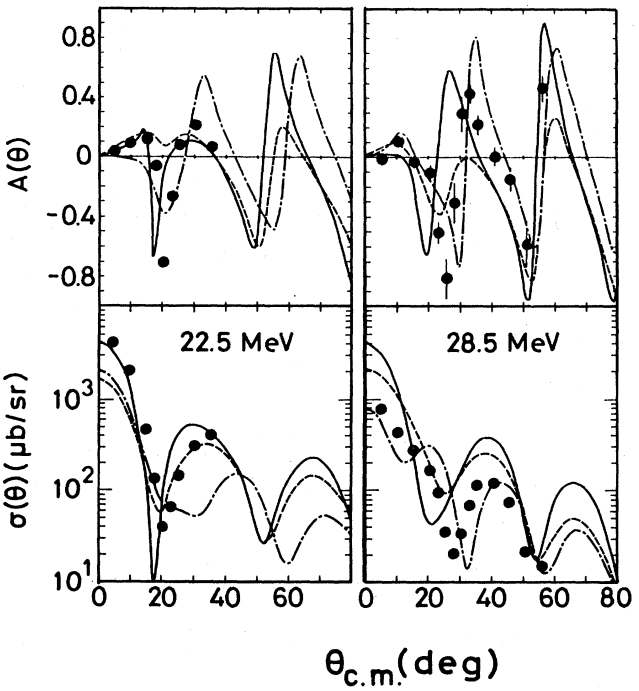

FIG. 1. (*Continued*).

III. ANALYSES IN TERMS OF THE FIRST- AND SECOND-ORDER DWBA

A. ^{92}Zr(p,t)^{90}Zr($0^+_{g.s.}$) reaction

In order to reproduce the data of the analyzing powers and cross sections for the reaction ^{92}Zr(p,t)^{90}Zr($0^+_{g.s.}$) shown in Fig. 1, we first made a first-order distorted-wave Born approximation (DWBA) calculation[27,28] in the zero-range approximation. We reasonably assumed that the nuclear structure involved in the one-step $N=52\rightarrow 50$ (p,t) transition is the $(d_{5/2})^2\rightarrow(d_{5/2})^0$ configuration. The form factor for the (p,t) transfer is calculated by the Bayman-Kallio method[29] with use of the single-particle neutron wave functions. The integration is performed numerically[30] and the correct asymptotic behavior of the form factor is obtained by giving the neutron binding energies, the sum of which equals the experimental two-neutron separation energy $S(2n)$ (Table II). We employed the optical potentials with parameters determined so as to reproduce both the cross section and polarization data of the elastic scattering of protons by Becchetti and Greenlees[31] and of tritons by Hardekopf *et al.*[32] (Table III). The energy dependence of the optical potential parameters for protons[31] is taken into account as shown in Table III, while the parameters for tritons[32] are fixed at $E_t=17$ MeV because there is no systematic study for the energy dependence of the optical potential parameters of tritons. It should be noted that the energy of the tritons in the reactions ^{92}Zr(p,t)^{90}Zr($0^+_{g.s.}$) and ^{138}Ba(p,t)^{136}Ba($0^+_{g.s.}$) at $E_p\approx 24$ MeV is nearly equal to $E_t\approx 17$ MeV.

The first-order DWBA calculations thus obtained are shown by dash-dotted curves in Fig. 1. The experimental analyzing powers are not reproduced at all by the one-step DWBA calculation, especially for the angular range around $\theta\approx 20°$ where the corresponding cross sections give the first minimum. The experimental analyzing powers around $\theta\approx 20°$ show a marked variation with incident proton energy, while the one-step DWBA calculation always predicts a sharp negative dip at $\theta\lesssim 20°$ and a successive sharp positive peak at $\theta\gtrsim 20°$, both of which yield a large discrepancy with the experimental analyzing powers. The discrepancy between the experiment and the calculation is

TABLE III. Optical-potential parameters[a] used in the first- and second-order DWBA calculations for the reactions ^{92}Zr(p,t)^{90}Zr($0^+_{g.s.}$) and ^{138}Ba(p,t)^{136}Ba($0^+_{g.s.}$). An energy E is the laboratory energy in MeV.

	Proton (^{92}Zr,^{138}Ba)	Deuteron 1 (^{91}Zr)	Deuteron 2 (^{91}Zr,^{137}Ba)	Triton 1 (^{90}Zr)	Triton 2 (^{90}Zr)	Triton 3 (^{136}Ba)
V_R	$54.0-0.32E+0.42A^{-1/3}$	$91.13+2.2ZA^{-1/3}$	$86-0.285E+0.88ZA^{-1/3}$	165.0	166.7	162.0
r_R	1.17	1.05	1.15	1.2	1.16	1.2
a_R	0.75	0.86	0.81	0.66	0.752	0.66
W_V	$9.1-0.03E+12(N-Z)/A$	0	0	13.8	23.3	13.4
W_D	$11.8-0.25E+12(N-Z)/A$	$218A^{-2/3}$	$15.9-0.9\exp(-E/91.7)$	0	0	0
$r_{V,D}$	1.32	1.43	1.31	1.6	1.498	1.6
$a_{V,D}$	$0.51+0.7(N-Z)/A$	$0.50+0.013A^{2/3}$	$0.495+0.064A^{1/3}$	0.80	0.819	0.99
V_{so}	6.2	3.5	$4.865/(1+0.0095E)^2$	6.0	0	6.0
r_{so}	1.01	0.75	1.10	1.10		1.10
a_{so}	0.75	0.50	0.55	0.40		0.80
r_C	1.25	1.3	1.30	1.30	1.25	1.3
Ref.	31	35	36	32	33	32

[a]Well depths in MeV and lengths in fm.

$$U(r)=-V_R f(x_R)-i[W_V f(x_V)-4W_D df(x_D)/dx_D]+2(\hbar/m_\pi c)^2(V_{so}/r)df(x_{so})/dr(\vec{l}\cdot\vec{s})+V_C\ ,$$

where

$$f(x_i)=(1+e^{x_i})^{-1},\quad x_i=(r-r_iA^{1/3})/a_i\ .$$

V_C is the Coulomb potential of a uniformly charged sphere of radius $r_CA^{1/3}$.

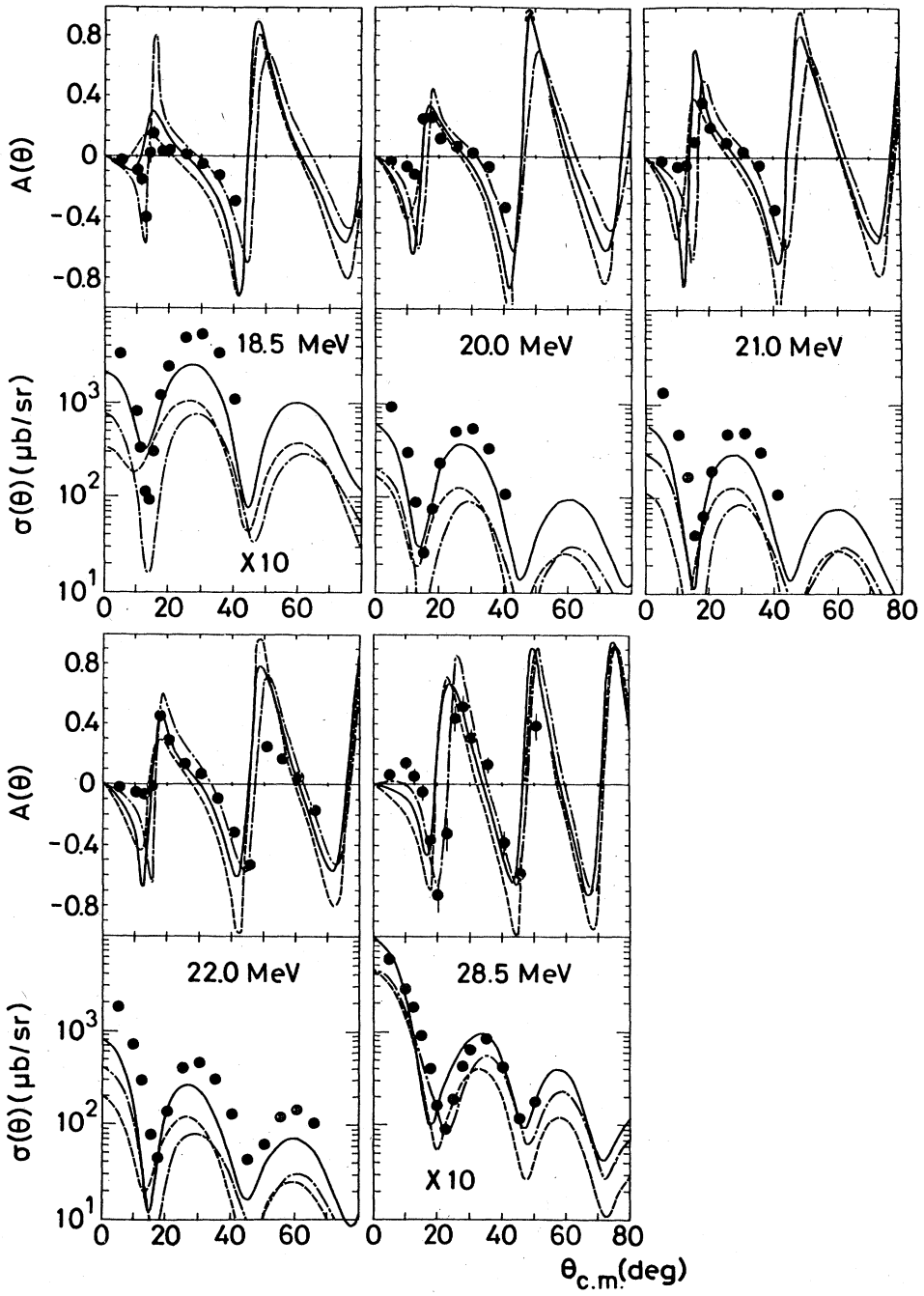

FIG. 2. Experimental and calculated analyzing powers $A(\theta)$ and cross sections $\sigma(\theta)$ for the reaction ^{138}Ba(p,t)^{136}Ba($0^+_{g.s.}$) at five proton energies in the laboratory system. The definition of curves are the same as that in Fig. 1. A factor of 10 is multiplied to both the experimental and calculated cross sections in the cases of $E_p = 18.5$ and 28.5 MeV.

found commonly over the whole energy range from $E_p = 17.0$ to 28.5 MeV.

Can we recover the failure in reproducing the experimental analyzing powers within the framework of the first-order DWBA by modifying some optical potential parameters in the proton and/or triton channels? The answer is no because a derivative relation between an analyzing power $A(\theta)$ and the corresponding cross section $\sigma(\theta)$

$$A(\theta) \approx [d\sigma(\theta)/d\theta]/\sigma(\theta) \quad (1)$$

is valid in good approximation for the present $0^+ \rightarrow 0^+$(p,t) transition within the framework of the first-order DWBA. The *plus-derivative rule* (1) is derived in the Appendix. According to this relation, a sharp oscillation with a negative dip and a successive positive peak in the analyzing power angular distribution must appear around $\theta \approx 20°$ as far as the first-order DWBA theory has once reproduced the first minimum in the cross section

angular distribution at $\theta \approx 20°$; see the dash-dotted curves in Fig. 1. This conclusion does not of course depend upon the optical potential parameters of the both proton and triton channels. Actually, we recalculated the analyzing power by replacing the triton optical potential of Hardekopf *et al.* with that of Flynn *et al.*[33] (Table III), which has no spin-orbit term. The resulting analyzing power is found to be quite similar to that given in Fig. 1 with the dash-dotted curves; see also Fig. 7 and Sec. IV B. In the present paper we call an analyzing power for a $0^+ \rightarrow 0^+$(p,t) transition as anomalous when its angular distribution deviates essentially from the derivative relation given by Eq. (1).

From the above-mentioned result it can be concluded that other reaction mechanisms than the direct one-step mechanism are essential to interpret the observed energy dependence of the (p,t) analyzing powers displaying anomalous angular distribution at $\theta \approx 20°$. Then we include sequential transfer (p,d)(d,t) two-step processes in terms of the second-order DWBA calculation.[28] We have already succeeded in interpreting the anomalous (p,t) analyzing powers for some $0^+_{g.s.} \rightarrow 0^+_{g.s.}$(p,t) transitions by taking into account the strong (p,d)(d,t) two-step processes.[1-4]

We employed the zero-range approximation in the first- and second-order DWBA calculations.[28] Finite-range effect on the analyzing powers and cross sections is discussed in Sec. IV C. Throughout the present calculations of the (p,d)(d,t) two-step processes, the deuterons in the intermediate channel are assumed to be their ground state. The effect of deuteron-unbound state channels is discussed in Sec. IV C. Also the effect of the nonorthogonal term, which is neglected in the present calculation, is discussed in Sec. IV C.

We have three zero-range normalization constants[28] D_0^2(p,t), D_0^2(p,d), and D_0^2(d,t) in our first- and second-order DWBA calculations. Concerning the normalization constants of the one-nucleon transfer processes (p,d) and (d,t), they can be experimentally well determined by utilizing the actual (p,d) and (d,t) reactions such as ^{92}Zr(p,d)^{91}Zr and ^{91}Zr(d,t)^{90}Zr. The following values are commonly used in the present analyses:

$$D_0^2(\mathrm{p,d}) = 1.53 \times 10^4, \quad D_0^2(\mathrm{d,t}) = 3.37 \times 10^4 , \tag{2}$$

in units of MeV^2 fm^3. Actually the above values of D_0^2(p,d) and D_0^2(d,t) have been successfully used in our analysis of the (p,d) and (d,t) reactions on the target nuclei of $A = 60$–208 at $E_p \approx 22$ MeV (Refs. 8 and 10) and at $E_d \approx 17$ MeV (Ref. 34). By employing these two values given by Eq. (2), the zero-range normalization D_0^2(p,t) of the one-step (p,t) term is determined experimentally. We take the absolute value of D_0^2(p,t) as an adjustable parameter of the one-step process to fit the experimentally observed absolute cross sections of the $0^+_{g.s.} \rightarrow 0^+_{g.s.}$(p,t) reactions in our first- and second-order DWBA calculations, since we explicitly include the (p,d)(d,t) two-step processes. Actually we fix the parameter value as

$$D_0^2(\mathrm{p,t}) = 22 \times 10^4 \ \ \mathrm{MeV^2\,fm^3} \tag{3}$$

throughout the present calculations; see Figs. 1 and 2. Thus we have no adjustable parameters for the relative amounts of the one- and two-step contributions in the present calculations.

Again we reasonably assumed that the nuclear structure involved in the two-step $N = 52 \rightarrow 51 \rightarrow 50$ transition is the

$$^{92}\mathrm{Zr}[0^+_{g.s.},(d_{5/2})^2] \rightarrow {}^{91}\mathrm{Zr}[\tfrac{5}{2}^+_{g.s.},(d_{5/2})^1] \rightarrow {}^{90}\mathrm{Zr}[0^+_{g.s.}(d_{5/2})^0]$$

configuration. We employed the deuteron optical potential of Lohr and Haeberli[35] except for the case of $E_p = 28.5$ MeV where the deuteron optical potential of Daehnick *et al.*[36] was used because the deuteron energy involved in the (p,d)(d,t) process is beyond the applicability of the potential of Lohr and Haeberli. The potential parameters used are given in Table III.

The calculated analyzing power $A(\theta)$ of the (p,d)(d,t) two-step processes, which are shown by dashed curves in Fig. 1, are quite different not only from the calculated one-step $A(\theta)$ but also from the experimental $A(\theta)$, especially around $\theta \approx 20°$. However, the coherent sum of the reaction amplitudes of the one- and two-step processes improves the fit to the experimental $A(\theta)$ drastically around $\theta \approx 20°$; see the solid curves in Fig. 1. The strong incident energy dependence of the experimental analyzing powers observed around $\theta \approx 20°$ is explained quite well in terms of a delicate interference effect between the one- and two-step processes. It should be emphasized that the interference between the one- and two-step processes is essential to reproduce the anomalous analyzing power. In addition to the analyzing power $A(\theta)$, the experimental cross sections $\sigma(\theta)$ are reproduced very well by inclusion of the both one- and two-step processes not only in their angular distributions but also in their absolute magnitudes; see the solid curves in the lower half of Fig. 1. It should be noted that the contribution of the (p,d)(d,t) two-step process is as much as that of the direct one-step process in the strong (p,t) g.s. transition.

B. ^{138}Ba(p,t)^{136}Ba($0^+_{g.s.}$) reaction

Measured analyzing powers and cross sections for the reaction ^{138}Ba(p,t)^{136}Ba($0^+_{g.s.}$) at $E_p = 18.5$, 20.0, 21.0, 22.0, and 28.5 MeV are shown in Fig. 2. The observed analyzing powers for ^{138}Ba(p,t)^{136}Ba always show a negative dip at $\theta \lesssim 15°$ and a successive positive peak at $\theta \gtrsim 15°$.

We carried out the first- and second-order DWBA calculation by assuming the similar reaction dynamics as in the case of the reaction ^{92}Zr(p,t)^{90}Zr($0^+_{g.s.}$) with use of the zero-range normalization constants D_0^2(p,d), D_0^2(d,t), and D_0^2(p,t) given by Eqs. (2) and (3). The nuclear structure involved in the reaction processes are assumed to be a mixed configuration of the neutron orbits of $d_{3/2}$, $s_{1/2}$, and $h_{11/2}$. This is because the three states exist very close with each other in the $N = 81$ nucleus ^{137}Ba as are shown in Fig. 3. In comparison we show the level structure of the $N = 51$ nucleus ^{91}Zr in Fig. 3. We calculated the configuration mixing of the nuclear-structure wave functions in terms of the monopole-pairing vibrational model.[40,41] The spectroscopic amplitudes thus obtained[42,43] for the reaction processes

^{138}Ba(p,d)^{137}Ba(d,t)^{136}Ba($0^+_{g.s.}$)

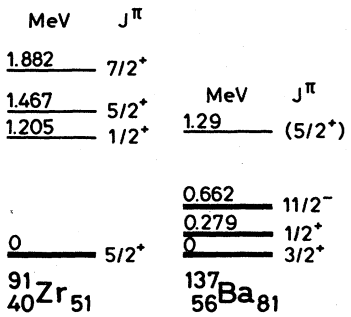

FIG. 3. Level structure of nuclei ^{91}Zr and ^{137}Ba (Ref. 47). The states which are taken into account as the intermediate states in the (p,d)(d,t) two-step calculations are indicated with bold lines.

and

$$^{138}\mathrm{Ba(p,d)}^{137}\mathrm{Ba(d,t)}^{136}\mathrm{Ba}(0^+_{\mathrm{g.s.}})$$

are given in Table IV. We employed the optical potential parameters for protons by Bechetti and Greenlees,[31] for deuterons by Daehnick *et al.*,[36] and for tritons by Hardekopf *et al.*;[32] see Table III.

Calculated analyzing powers $A(\theta)$ and cross sections $\sigma(\theta)$ are compared with the experimental results in Fig. 2. The calculated two-step $A(\theta)$ (dashed curves) are quite similar to the calculated one-step $A(\theta)$ (dash-dotted curves). In consequence the resultant total $A(\theta)$ (solid curves) obtained from the coherent sum of the two processes are just like the one-step $A(\theta)$. The theoretical analyzing powers thus obtained are completely different from those for the reaction ^{92}Zr(p,t)^{90}Zr and consequently can explain the characteristic features of the experimental analyzing powers for the reaction ^{138}Ba(p,t)^{136}Ba given by items (iii) and (iv) well, i.e., the analyzing powers with no marked change with incident proton energy and those without anomalous angular distribution.

In addition to the analyzing powers, the experimental cross sections are reproduced in terms of the first- and second-order DWBA calculation well; the final results are shown by solid curves. The two-step contribution, which is as large as the one-step one, interferes with the one-step contribution *constructively* so that the final cross section obtained by a coherent sum of the two processes becomes large enough to reproduce the magnitude of the experimental cross section; see the lower half of Fig. 2.

Contributions of the three neutron orbits $d_{3/2}$, $s_{1/2}$, and $h_{11/2}$ to the two-step processes

$$^{138}\mathrm{Ba(p,d)}^{137}\mathrm{Ba(d,t)}^{136}\mathrm{Ba}(0^+_{\mathrm{g.s.}})$$

are explained in Fig. 4 for the case of $E_p=22.0$ MeV. The behavior of the three orbits in the cases of the other proton energies is similar to that shown in Fig. 4. The contribution to the $h_{11/2}$ orbit, whose mixing amplitude A_{pdt} is the second largest as is shown in Table IV, is much suppressed due to its large centrifugal potential barrier for double $l=5$ neutron transfers in the

$$^{138}\mathrm{Ba(p,d)}^{137}\mathrm{Ba(d,t)}^{136}\mathrm{Ba}(0^+_{\mathrm{g.s.}})$$

process. Indeed Fig. 4 demonstrates that the partial cross

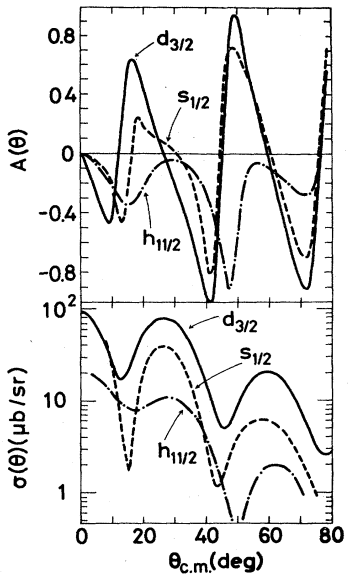

FIG. 4. Contributions of the three neutron orbits $d_{3/2}$, $s_{1/2}$, and $h_{11/2}$ to the two-step processes ^{138}Ba(p,d)^{137}Ba(d,t)^{136}Ba$(0^+_{\mathrm{g.s.}})$ in the case of $E_p=22.0$ MeV.

section of the $h_{11/2}$ orbit is smaller than that of the $d_{3/2}$ orbit by one order in magnitude. Since the $s_{1/2}$ orbit is a special case of $l=0$, i.e., $j_>=j_<=\frac{1}{2}$, the dominance of the $d_{3/2}$ orbit in the two-step process of the reaction ^{138}Ba(p,t)^{136}Ba$(0^+_{\mathrm{g.s.}})$ tells us that the most active orbit in this reaction can be considered to be a $j_<$ $(=d_{3/2})$ orbit.

IV. DISCUSSION

A. *J* dependence of analyzing powers

In order to demonstrate the principle that the j dependence of the (p,d)(d,t) two-step analyzing powers plays an essential role in producing the marked change of the ^{92}Zr(p,t) analyzing powers with proton energy on one hand and the nonvariation of the ^{138}Ba(p,t) analyzing powers on the other hand, we recalculate the ^{92}Zr(p,t) analyzing powers over the energy range from $E_p=17.0$ to 28.5 MeV in terms of the first- and second-order DWBA by changing the active neutron orbit from $d_{5/2}$ to $d_{3/2}$. The result is shown in Fig. 5. A comparison of Fig. 5 with Fig. 1 tells us the following:

(1) The two-step $A(\theta)$ obtained from $d_{3/2}$ is quite different from that from $d_{5/2}$; the two analyzing powers are out-of-phase with each other in angular distributions at

TABLE IV. Spectroscopic amplitudes A_{pt} and A_{pdt} for the one-step and the two-step (p,d)(d,t) processes, respectively, in the reaction ^{138}Ba(p,t)^{136}Ba$(0^+_{\mathrm{g.s.}})$.

	A_{pt}	A_{pdt}
$d_{3/2}$	0.666	0.942
$s_{1/2}$	0.373	0.527
$h_{11/2}$	0.646	0.913

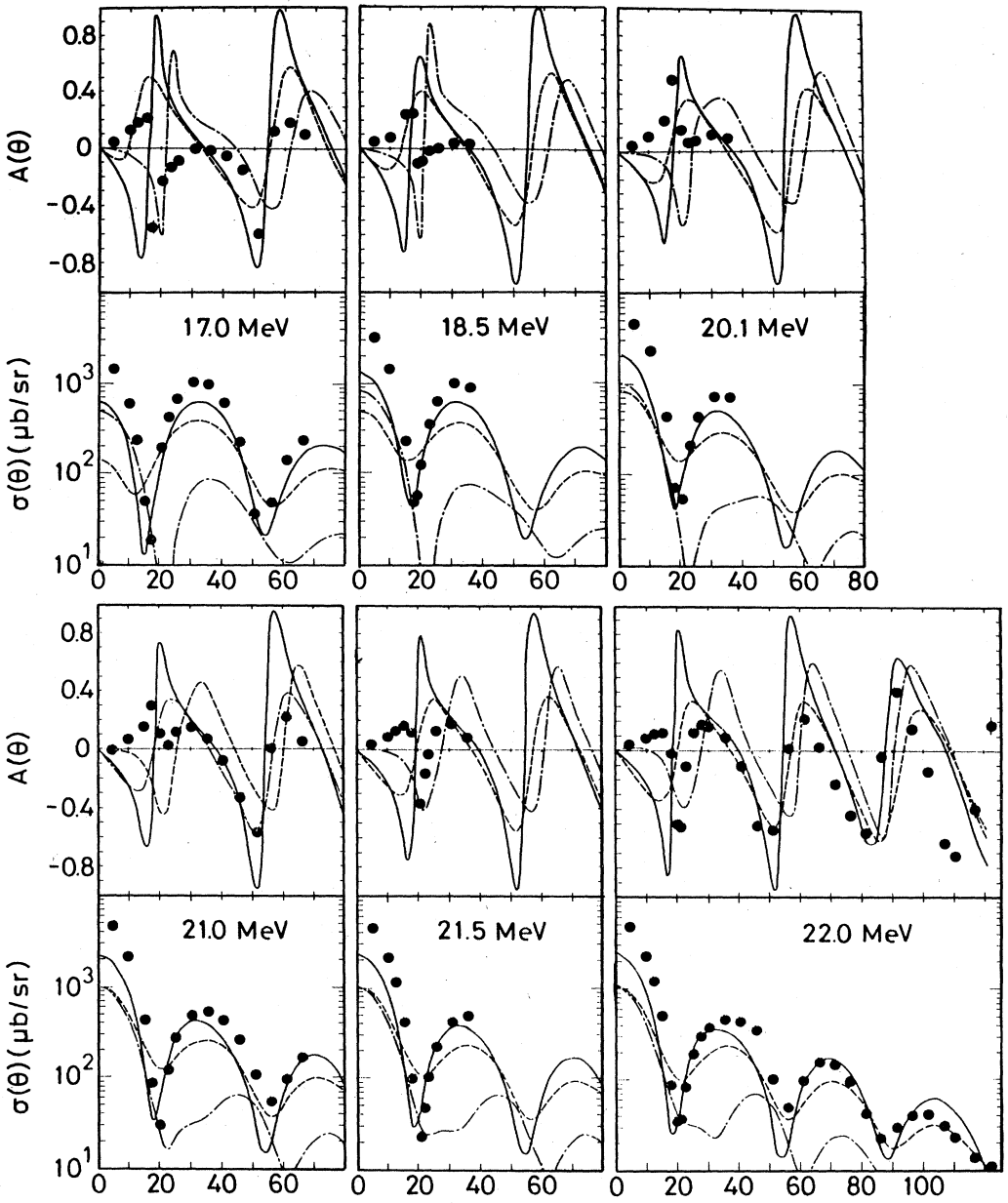

FIG. 5. Similar to Fig. 1, except for replacing the $(d_{5/2})^n$ configuration by the $(d_{3/2})^n$ one.

forward angles.

(2) The one-step $A(\theta)$ obtained from $d_{3/2}$ is very similar to that from $d_{5/2}$.

(3) The total $A(\theta)$ calculated from the coherent sum of the two processes in the case of $d_{3/2}$ is thus quite different from the total $A(\theta)$ in the case of $d_{5/2}$ at forward angles of $\theta \lesssim 30°$.

(4) In consequence, the $d_{3/2}$ analyzing powers (Fig. 5) do not explain at all the marked energy variation of the observed analyzing powers for the reaction ^{92}Zr(p,t)^{90}Zr; the $d_{3/2}$ calculation always predicts "normal" analyzing powers in the angular region where the cross sections give the first minimum.

The origin of the distinguished difference in the two-step analyzing powers between the $j_>$ and $j_<$ orbits has been discussed by Kubo[16] in the case of the analyzing-power experiment ^{144}Nd(p,t)^{142}Nd done by the Tsukuba group;[2] a comparison of $f_{7/2}$ with $f_{5/2}$ orbits has been made. We now show, in Fig. 6, the difference in the two-step $A(\theta)$ for the cases of the $j_>$ $(=d_{5/2})$ and $j_<$ $(=d_{3/2})$ orbits in the reaction ^{92}Zr(p,t)^{90}Zr$(0^+_{g.s.})$ at $E_p = 22.0$ MeV. Figure 6(a) shows shell-orbit dependence of calculated two-step analyzing powers without spin-orbit distortions for proton, deuteron, and triton channels. The oscillations of the two analyzing powers $A(\theta, j_>)$ and $A(\theta, j_<)$ are completely out of phase. Indeed it can be easily proved[16] by using geometrical properties of the transition amplitude[38] that the analyzing power for the

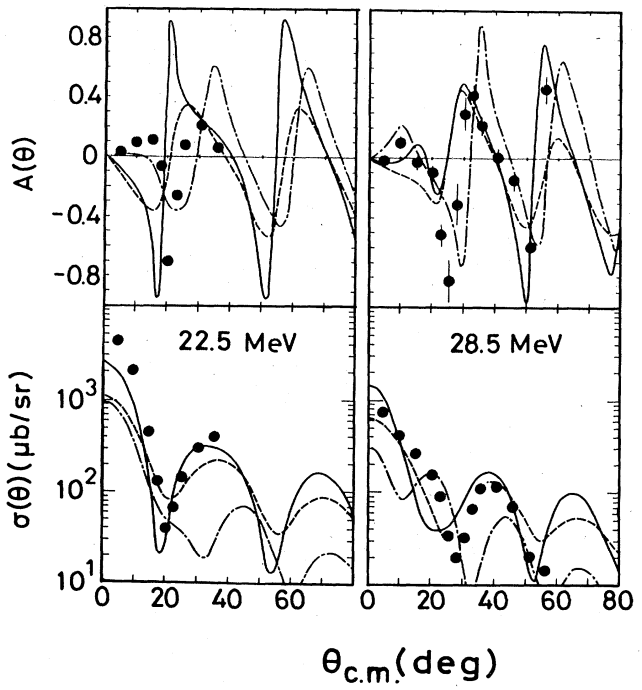

FIG. 5. (*Continued*).

two-step (p,d)(d,t) sequential transfer in the case of $0^+ \rightarrow 0^+$(p,t) transition changes its sign depending upon picking up from the neutron orbit $j_> = l + \frac{1}{2}$ or $j_< = l - \frac{1}{2}$, and the ratio of the two analyzing powers is expressed as

$$\frac{A(\theta, j_>)}{A(\theta, j_<)} = -\frac{l}{l+1}, \tag{4}$$

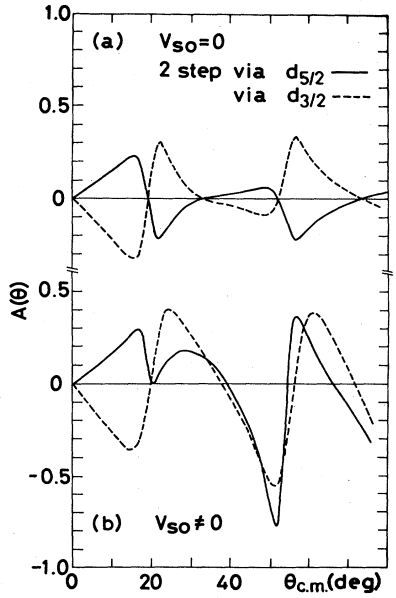

FIG. 6. Shell orbit dependence of calculated two-step analyzing powers for the cases of the $d_{5/2}$ and $d_{3/2}$ orbits in the reaction ^{92}Zr(p,t)^{90}Zr($0^+_{g.s.}$) at $E_p = 22.0$ MeV (a) without spin-orbit distortion and (b) with that distortion.

where l and j denote the orbital and the total angular momentum, respectively, from which two neutrons are picked up sequentially. In the case of Fig. 6(a), Eq. (4) becomes $A(\theta, d_{5/2})/A(\theta, d_{3/2}) = -\frac{2}{3}$. It should be noticed that the j dependence of the analyzing powers expressed by Eq. (4) is similar to that appearing in one-nucleon transfer reactions.[27,44] When spin-orbit distortions are included as in the actual case (the potential set Proton, Deuteron 1, and Triton 1 in Table III), such a simple rule described by Eq. (4) is violated, as can be seen in Fig. 6(b). However, the two analyzing powers show still opposite-phase oscillations at forward angles $\theta \lesssim 20°$ where the distortion effect is negligibly small.

The j dependence of the two-step analyzing powers, which is demonstrated by Fig. 6, can explain all the characteristic features given by items (i) to (v) in Sec. II. When two neutrons are picked up sequentially from a $j_>$ orbit, the two-step $A(\theta)$ is quite different from the one-step $A(\theta)$, so that the total $A(\theta)$ shows a completely different angular distribution from the one-step $A(\theta)$ in the forward angles. The interference effect between the one- and two-step processes is very sensitive to the relative phase between the transition amplitudes of the two processes. Therefore the (p,t) analyzing power shows a marked change with incident proton energy. On the other hand, when the two neutrons are picked up from the $j_<$ orbit, the two-step $A(\theta)$ is very similar to the one-step $A(\theta)$. The interference between the one- and two-step processes is thus quite stable against the relative phase of the transition amplitudes of the two processes. Therefore the (p,t) analyzing power shows a quite stable behavior in angular distributions with respect to the variation of the proton energy.

B. Optical potential parameters

Of the optical potentials employed in the present calculations for the (p,t) and the (p,d)(d,t) processes, the triton optical potential is the only case in which a systematic and global study of the optical potential by means of elastic scattering data is insufficient. Therefore, we need to examine carefully the effect of the parameter values of the triton optical potential on the (p,t) analyzing-power calculations. Actually we recalculate the energy dependence of the analyzing power for the reaction ^{92}Zr(p,t)^{90}Zr($0^+_{g.s.}$) by changing the triton potential from the Hardekopf potential[32] (set Triton 1 in Table III) to the Flynn potential[33] (set Triton 2). It should be noticed that the former potential has a spin-orbit term while the latter one has not. The result is shown in Fig. 7 for the incident proton energies of $E_p = 16$, 19, and 22 MeV. No appreciable change in the analyzing powers is found between the two cases. Therefore we can confirm the result of the first- and second-order calculations described in Sec. III.

C. Effects of finite-range interaction, nonorthogonal term, and deuteron-breakup channel

All the present calculations have been carried out in terms of the zero-range (ZR) DWBA by using the three normalization constants given by Eqs. (2) and (3). Now we have the following questions: Firstly, is the total

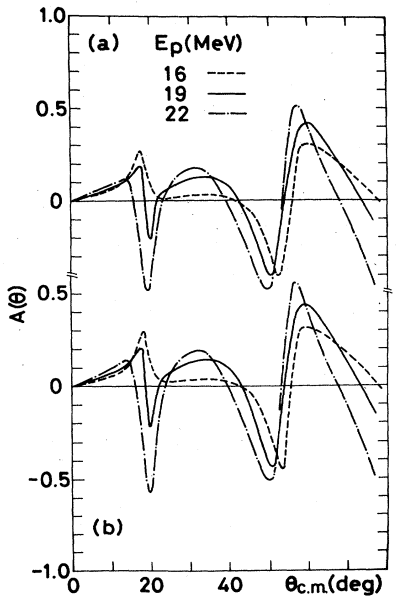

FIG. 7. Incident energy dependence of the calculated analyzing powers in terms of the first- and second-order DWBA for the reaction ^{92}Zr(p,t)^{90}Zr($0^+_{g.s.}$). (a) [(b)] employs the triton optical potential with [without] the spin-orbit term, i.e., set Triton 1 [Triton 2] in Table III.

analyzing power for the (p,t) reactions predicted in terms of the first- and second-order finite-range (FR)-DWBA calculations nearly equal to that obtained in the present ZR-DWBA calculations? Secondly, can the first- and second-order FR-DWBA calculations reproduce the absolute magnitude of the experimental cross sections for the (p,t) reactions without using any adjustable parameters?

Another important approximation which has been made in the present calculations is that a deuteron exists only in its ground state in the intermediate channels of (p,d)(d,t) processes, i.e., unbound deuteron intermediate channels or deuteron-breakup channels can be neglected. However, Pinkston and Satchler[45] have casted a doubt on this approximation. They have pointed out by employing the closure approximation that the analyzing power associated with (p,d)(d,t) transitions could be completely modified when the deuteron unbound ($S=0$, $T=1$) state is included in the two-step calculation.

In order to answer the above-mentioned questions, the first- and second-order FR-DWBA calculations including the deuteron unbound intermediate channels have been recently carried out for the case of the (p,t) experiment on the ^{208}Pb target at $E_p=22$ MeV (Refs. 7, 21, and 46) and $E_p=35$ and 50 MeV (Ref. 21): the natural-parity transition ^{208}Pb($\vec{p}$,t)^{206}Pb($0^+_{g.s.}$) and the unnatural-parity transition

$$^{208}\mathrm{Pb}(\vec{p},t)^{206}\mathrm{Pb}(3^+,1.34\ \mathrm{MeV})\ .$$

The FR calculation has explained both the experimental analyzing powers and the cross sections very well. The absolute values of the (p,t) cross sections have been reproduced quite well. It should be emphasized that the predicted $A(\theta,0^+_{g.s.})$ and $\sigma(\theta,0^+_{g.s.})$ in terms of the FR-DWBA calculations including the unbound deuteron intermediate channels are quite similar to those obtained from the ZR-DWBA calculations without including the unbound deuteron channels.[15] In addition, a large contribution of the (p,d)(d,t) two-step processes in the strong $0^+_{g.s.}\rightarrow 0^+_{g.s.}$(p,t) transition is confirmed again. The contribution from the unbound deuteron channels is found to be rather small at $E_p=22$ MeV. We can thus justify the use of the simple ZR-DWBA without including the unbound deuteron channels in carrying out analyses of the (p,t) data at $E_p=20$–30 MeV.

The two step cross section due to the nonorthogonal term[28] has been found much smaller than that due to the interaction term[28] by a factor of $\frac{1}{20}$ (Refs. 15 and 46). Therefore, the present calculations in which the nonorthogonal term is neglected because of the simplicity of the calculation can be justified.

V. CONCLUSION

Incident-energy dependence of analyzing powers $A(\theta)$ and cross sections $\sigma(\theta)$ were measured systematically for the $0^+_{g.s.}\rightarrow 0^+_{g.s.}$(p,t) reactions on the targets ^{92}Zr and ^{138}Ba which are around neutron-singly closed shell. A so-called anomalous analyzing power which does not satisfy the derivative relation $A(\theta)\simeq[d\sigma(\theta)/d\theta]/\sigma(\theta)$ is observed in the reaction ^{92}Zr(p,t)^{90}Zr($0^+_{g.s.}$) and a strong incident-energy dependence of the analyzing power is found. On the other hand, neither the "anomaly" nor the distinct incident-energy dependence is observed in the reaction ^{138}Ba(p,t)^{136}Ba($0^+_{g.s.}$).

The above-mentioned phenomena are explained as the nuclear-shell orbit dependence (j dependence) of the analyzing power for a (p,d)(d,t) two-step process. The analyzing powers for the $0^+_{g.s.}\rightarrow 0^+_{g.s.}$(p,t) transitions are classified into two types according to picking-up neutrons sequentially from a shell of $j_>=l+\frac{1}{2}$ or from a shell of $j_<=l-\frac{1}{2}$. In the first case, which corresponds to the $j_>=d_{5/2}$ in ^{92}Zr(p,t)^{90}Zr, the analyzing power for the (p,t) one-step process and that for the (p,d)(d,t) sequential two-step transfer process show opposite-phase angular oscillations with each other at forward angles. Consequently, a delicate interference effect between the one- and the two-step reaction amplitudes produces the anomaly and then the strong incident-energy dependence can be explained from this interference. On the contrary, in the second case, which corresponds to the $j_<=d_{3/2}$ in ^{138}Ba(p,t)^{136}Ba, the analyzing power for the (p,d)(d,t) two-step process is quite similar to that for the (p,t) one-step process. The total analyzing power is therefore normal and a marked incident-energy dependence of the analyzing power does not appear.

The present study demonstrates that strong $0^+_{g.s.}\rightarrow 0^+_{g.s.}$(p,t) transitions are explained from the existence of intense (p,d)(d,t) two-step processes which are as strong as the (p,t) one-step process. The (p,t) analyzing-power measurement enables us to obtain this conclusion.

ACKNOWLEDGMENTS

We would like to thank Dr. T. Hasegawa of INS for supporting our experiment at INS, and Dr. K.-I. Kubo and Dr. T. Kishimoto for their helpful discussions and suggestions on the theoretical problems.

APPENDIX: DERIVATIVE RELATION

We now show that the derivative relation expressed by Eq. (1) between the vector analyzing power $A(\theta)$ and the differential cross section $\sigma(\theta)$ in the (p,t) transition of $0^+\rightarrow 0^+$ is derived in terms of the first-order DWBA theory. This relation does not depend on whether the zero-range or the finite-range interaction is employed. In this appendix, we use the zero-range approximation.

First of all, the vector analyzing power $A(\theta)$ and the cross section $\sigma(\theta)$ can be expressed in the following way in terms of the transition amplitudes $B_j^{m\sigma_f\sigma_i}$ (Refs. 27 and 38):

$$A(\theta)=-\frac{\sum_{jm\sigma_f\sigma_i}[(s_i+\sigma_i+1)(s_i-\sigma_i)]^{1/2}\mathrm{Im}(B_j^{m\sigma_f\sigma_i}B_j^{m-1\sigma_f\sigma_i+1*})}{s_i\sum_{jm\sigma_f\sigma_i}|B_j^{m\sigma_f\sigma_i}|^2}, \tag{A1}$$

$$\sigma(\theta)=\frac{\mu_i\mu_f}{(2\pi\hbar^2)^2}\frac{k_f}{k_i}\frac{2J_f+1}{(2J_i+1)(2s_i+1)}\sum_{jm\sigma_f\sigma_i}|B_j^{m\sigma_f\sigma_i}|^2, \tag{A2}$$

where the incident (outgoing) particle has a spin s_i (s_f), and the target (residual) nuclear spin is J_i (J_f). The magnetic quantum number of the spin s_i, s_f, J_i, and J_f is σ_i, σ_f, M_i, and M_f, respectively. In addition, we define the transfer angular momenta as

$$\vec{j}=\vec{J}_f-\vec{J}_i,\quad \vec{s}=\vec{s}_i-\vec{s}_f,\quad \vec{l}=\vec{j}-\vec{s}, \tag{A3}$$

and

$$m=M_f-M_i+\sigma_f-\sigma_i. \tag{A4}$$

The μ_i and μ_f are the reduced masses of the incident and outgoing channel, respectively, and k_i and k_f are the relative momenta of the respective channels. Usually the transition amplitude $B_j^{m\sigma_f\sigma_i}$ is divided into a spectroscopic amplitude $A_{lsj}^{J_fJ_i}$ and a reduced amplitude $\beta_{lsj}^{m\sigma_f\sigma_i}(\theta)$:

$$B_j^{m\sigma_f\sigma_i}=A_{lsj}^{J_fJ_i}\beta_{lsj}^{m\sigma_f\sigma_i}(\theta). \tag{A5}$$

The reduced amplitude $\beta_{lsj}^{m\sigma_f\sigma_i}$ satisfies generally the following relation:[27,38]

$$\beta_{lsj}^{m\sigma_f\sigma_i}(\theta)=(-)^{m+j+l+s_f-s_i}\beta_{lsj}^{-m-\sigma_f-\sigma_i}(\theta). \tag{A6}$$

In the $0^+\rightarrow 0^+$(p,t) transition, we have $l=s=j=0$ and $s_i=s_f=\frac{1}{2}$. Then Eq. (A6) becomes

$$\beta^{m\sigma_f\sigma_i}(\theta)=(-)^m\beta^{-m-\sigma_f-\sigma_i}, \tag{A7}$$

where we drop the l, s, and j because they are unique. By using the above relations, the differential cross section in Eq. (A2) can be written as

$$\sigma(\theta)=K[\,|B^{0(1/2)(1/2)}(\theta)|^2+|B^{1(1/2)(-1/2)}(\theta)|^2], \tag{A8}$$

where

$$K\equiv\frac{\mu_i\mu_f}{(2\pi\hbar^2)^2}\frac{k_f}{k_i}\frac{2J_f+1}{2J_i+1}. \tag{A9}$$

From Eq. (A1), the analyzing power is written as

$$A(\theta)=\frac{2\,\mathrm{Im}[B^{0(1/2)(1/2)}(\theta)B^{1(1/2)(-1/2)}(\theta)^*]}{|B^{0(1/2)(1/2)}(\theta)|^2+|B^{1(1/2)(-1/2)}(\theta)|^2}. \tag{A10}$$

The explicit form of the transition amplitude is given by[27,38]

$$B_j^{m\sigma_f\sigma_i}(\theta)=\sum_{ls}A_{lsj}^{J_fJ_i}\sum_{\substack{L_bJ_b\\L_aJ_a}}i^{L_a-L_b-l}\left[\frac{(L_b-m)!}{(L_b+m)!}\right]^{1/2}\begin{Bmatrix}j & l & s\\ J_a & L_a & s_i\\ J_b & L_b & s_f\end{Bmatrix}$$

$$\times P_{L_b}^m(\cos\theta)I_{L_bJ_b,L_aJ_a}^{lsj}\hat{L}_b\hat{l}\hat{s}\hat{L}_a\hat{J}_b(J_b\sigma_f-mjm-\sigma_f+\sigma_i\,|\,J_a\sigma_i)$$

$$\times(L_a0s_i\sigma_i\,|\,J_a\sigma_i)(L_b-ms_f\sigma_f\,|\,J_b\sigma_f-m)(L_b0l0\,|\,L_a0), \tag{A11}$$

where L_a (L_b) and J_a (J_b) are the orbital and the total angular momentum of the initial (final) partial wave, respectively, and $\hat{x}$ stands for $(2x+1)^{1/2}$. When $l=s=j=0$, we have $L_a=L_b\equiv L$, $J_a=J_b\equiv J$ because of the property of vector coupling. In this case, the radial integral $I_{L_bJ_b,L_aJ_a}^{lsj}$ is reduced to the form of

$$I_{LJ}=\frac{2\pi^{1/2}}{k_ik_f}\frac{B}{A}\int\chi_{LJ}^{(f)}\left(\frac{A}{B}r\right)F_0(r)\chi_{LJ}^{(i)}(r)dr, \tag{A12}$$

where A and B are the masses of the target and the residual nucleus, respectively, and χ_{LJ} is the distorted partial wave. The $F_0(r)$ is the radial part of the form factor of the $0^+ \rightarrow 0^+$(p,t) one-step transition.

We consider the spin-orbit force (the $\vec{L}\cdot\vec{\sigma}$ interaction) as a perturbation to the main central force. Thus we can assume that the spin-orbit force affects only the phase shift of each partial wave in such a way as

$$\chi_{LJ} \approx \tilde{\chi}_L \exp(iC_L \langle \vec{L}\cdot\vec{\sigma} \rangle) , \tag{A13}$$

where

$$\langle \vec{L}\cdot\vec{\sigma} \rangle = \begin{cases} L & \text{for } J = L + \frac{1}{2} , \\ -L-1 & \text{for } J = L - \frac{1}{2} . \end{cases} \tag{A14}$$

The $\tilde{\chi}_L$ is a partial wave in the case of non-spin-orbit coupling and then it is independent of J. The C_L is a small parameter related to the sign and the strength of the spin-orbit force. By inserting Eq. (A13) into Eq. (A12), we obtain

$$I_{LJ} = \exp(i\bar{C}_L \langle \vec{L}\cdot\vec{\sigma} \rangle) \tilde{I}_L , \tag{A15}$$

where $\tilde{I}_L$ is the radial integral in terms of $\tilde{\chi}_L$, and $\bar{C}_L$ is the sum of the two C_L's for the incident and outgoing channels.

From Eq. (A11), we have

$$B^{0(1/2)(1/2)}(\theta) = \frac{A_0}{2\sqrt{2}} \sum_{LJ} (2J+1) I_{LJ} P_L(\cos\theta) \tag{A16}$$

and

$$B^{1(1/2)(-1/2)}(\theta) = \frac{A_0}{\sqrt{2}} \sum_{LJ} (-)^{J-L-(1/2)} I_{LJ} P_L^1(\cos\theta) , \tag{A17}$$

where A_0 denotes the spectroscopic amplitude. By inserting Eq. (A15) into Eqs. (A16) and (A17), and applying a Taylor expansion for the exponent in Eq. (A15), we obtain the following result in the first-order approximation for $\bar{C}_L$:

$$B^{0(1/2)(1/2)}(\theta) = \frac{A_0}{\sqrt{2}} \sum_{L} (2L+1) \tilde{I}_L P_L(\cos\theta) \tag{A18}$$

and

$$B^{1(1/2)(-1/2)}(\theta) = \frac{i}{\sqrt{2}} A_0 \sum_{L} \bar{C}_L (2L+1) \tilde{I}_L P_L^1(\cos\theta) . \tag{A19}$$

If we assume that the $\bar{C}_L$ is effective only for a few L values, we can take it outside the summation over L and thus replace it by its average value $\bar{C}$. This procedure is reasonable under the assumption of the direct-nuclear-reaction mechanism where the nuclear reaction takes place mainly around the nuclear surface. The above-mentioned procedure is similar to that used by Johnson.[39] Then we have the following relation by comparing Eq. (A18) with (A19):

$$\frac{d}{d\theta} B^{0(1/2)(1/2)}(\theta) = \frac{i}{\bar{C}} B^{1(1/2)(-1/2)}(\theta) , \tag{A20}$$

because we know the following relation between a Legendre function and an associated Legendre function:

$$\frac{d}{d\theta} P_L(\cos\theta) = -P_L^1(\cos\theta) . \tag{A21}$$

In the expression for the cross section of Eq. (A8), the first term of the right-hand side is dominant because the second term is proportional to C^2 due to Eq. (A19) and thus can be neglected in our first-order approximation. It is well-known that the first (second) term corresponds to a spin-nonflip (spin-flip) process. In this approximation we have

$$\sigma(\theta) \approx K \, | \, B^{0(1/2)(1/2)}(\theta) \, |^2 . \tag{A22}$$

By inserting Eqs. (A20) and (A22) into Eq. (A10), we obtain the final result:

$$A(\theta) \approx \bar{C} \frac{d}{d\theta} \sigma(\theta) / \sigma(\theta) . \tag{A23}$$

It should be noted that the derivative rule actually observed in our $0^+ \rightarrow 0^+$(p,t) transitions is the *plus-derivative rule* as expressed by Eq. (1), i.e., $\bar{C} > 0$ in Eq. (A23). This can be explained in the following way. The spin-orbit term in the optical potential both for protons and tritons is negative[48] in the nuclear surface region as shown in Table III. This means that the spin-orbit potential is attractive[48] for both protons and tritons. Therefore, we obtain positive[48] (advanced) phase shifts for some effective partial waves of both protons and tritons. Thus we have the relation $C_L > 0$ in Eq. (A13) for the partial waves, which results in the relation $\bar{C} > 0$ in Eq. (A23).

The plus-derivative rule expressed by Eq. (1) is well-known in the case of polarization phenomena in elastic scattering experiments, see, e.g., p. 437 of Ref. 38.

---

*Present address: Research Institute for Brain and Blood Vessels—Akita, Senshukubota-Machi, Akita 010, Japan.

[1]K. Yagi, in *Polarization Phenomena in Nuclear Physics—1980 (Fifth International Symposium, Sante Fe)*, Proceedings of the Fifth International Symposium on Polarization Phenomena in Nuclear Physics, AIP Conf. Proc. No. 69, edited by G. G. Ohlson, R. E. Brown, N. Jarmie, M. W. McNaughton, and G. M. Hale (AIP, New York, 1981), p. 254.

[2]K. Yagi, S. Kunori, Y. Aoki, K. Nagano, Y. Toba, and K.-I. Kubo, Phys. Rev. Lett. **43**, 1087 (1979).

[3]Y. Toba, Y. Aoki, S. Kunori, K. Nagano, and K. Yagi, Phys. Rev. C **20**, 1204 (1979).

[4]S. Kunori, Y. Aoki, H. Iida, K. Nagano, Y. Toba, and K. Yagi, Phys. Rev. Lett. **46**, 810 (1981).

[5]Y. Aoki, H. Iida, S. Kunori, K. Nagano, Y. Toba, and K Yagi, Phys. Rev. C **25**, 1050 (1982).

[6]Y. Aoki, H. Iida, S. Kunori, K. Nagano, Y. Toba, and K. Yagi, Phys. Rev. C **25**, 1696 (1982).

[7]M. Igarashi and K.-I. Kubo, Phys. Rev. C **25**, 2144 (1982).
[8]Y. Toba, K. Nagano, Y. Aoki, S. Kunori, and K. Yagi, Nucl. Phys. **A359**, 76 (1981).
[9]K. Nagano, Y. Aoki, H. Iida, S. Kunori, Y. Toba, and K. Yagi, in *Polarization Phenomena in Nuclear Physics—1980 (Fifth International Symposium, Sante Fe),* Proceedings of the Fifth International Symposium on Polarization Phenomena in Nuclear Physics, AIP Conf. Proc. No. 69, edited by G. G. Ohlson, R. E. Brown, N. Jarmie, M. W. McNaughton, and G. M. Hale (AIP, New York, 1981), p. 617.
[10]Y. Aoki, H. Iida, K. Nagano, Y. Toba, and K. Yagi, Nucl. Phys. **A393**, 52 (1983).
[11]H. Iida, Y. Aoki, K. Hashimoto, K. Nagano, Y. Tagishi, Y. Toba, and K. Yagi, Phys. Rev. C **29**, 328 (1984).
[12]K. Yagi, S. Kunori, Y. Aoki, Y. Higashi, J. Sanada, and Y. Tagishi, Phys. Rev. Lett. **40**, 161 (1978).
[13]K. Yagi, S. Kunori, Y. Aoki, K. Nagano, Y. Tagishi, and Y. Toba, Phys. Rev. C **19**, 285 (1979).
[14]K. Yagi, S. Kunori, Y. Aoki, K. Nagano, Y. Tagishi, and Y. Toba, *Proceedings of the Institute for Nuclear Study International Symposium on Direct Reaction Mechanism, Fukuoka, 1978* (Institute for Nuclear Study, University of Tokyo, 1978), p. 137.
[15]Y. Toba, Y. Aoki, H. Iida, S. Kunori, K. Nagano, and K. Yagi, Phys. Lett. **100B**, 232 (1981).
[16]K.-I. Kubo, Phys. Rev. C **23**, 2753 (1981).
[17]Y. Aoki, H. Iida, K. Hashimoto, K. Nagano, M. Takei, Y. Toba, and K. Yagi, Nucl. Phys. **A394**, 413 (1983).
[18]K. Nagano, Y. Aoki, T. Kishimoto, and K. Yagi, Nucl. Phys. (to be published).
[19]Y. Aoki, S. Kunori, K. Nagano, Y. Toba, and K. Yagi, J. Phys. Soc. Jpn. **47**, 329 (1979).
[20]Y. Aoki, S. Kunori, K. Nagano, Y. Toba, and K. Yagi, Nucl. Phys. **A382**, 269 (1982).
[21]K. Yagi, Y. Aoki, K. Hashimoto, H. Iida, H. Sakamoto, Y. Tagishi, M. Matoba, M. Igarashi, and K.-I. Kubo, Phys. Rev. C (to be published).
[22]Y. Tagishi and J. Sanada, Nucl. Instrum. Methods **164**, 411 (1979).
[23]J. E. Spencer and H. A. Enge, Nucl. Instrum. Methods **49**, 181 (1967).
[24]H. Iida, Y. Aoki, K. Yagi, and M. Matoba, Nucl. Instrum. Methods **224**, 432 (1984).
[25]S. Kato, T. Hasegawa, and M. Tanaka, Nucl. Instrum. Methods **154**, 19 (1978).
[26]K. Iwata, H. Yokomizo, M. Tanaka, S. Kato, T. Hasegawa, H. Hasai, and F. Nishiyama, Nucl. Instrum. Methods **171**, 61 (1980).
[27]G. R. Satchler, Nucl. Phys. **55**, 1 (1964).
[28]H. Hashimoto and M. Kawai, Prog. Theor. Phys. **59**, 1265 (1978); N. Hashimoto, *ibid.* **59**, 1562 (1978).
[29]B. F. Bayman and K. Kallio, Phys. Rev. C **1**, 976 (1970).
[30]M. Igarashi, computer code TWOFNR/PTFF (unpublished).
[31]F. D. Becchetti, Jr. and G. W. Greenlees, Phys. Rev. **182**, 1190 (1969).
[32]R. A. Hardekopf, R. F. Haglund, G. G. Ohlsen, W. J. Thompson, and L. R. Veeser, Phys. Rev. C **21**, 906 (1980).
[33]E. R. Flynn, D. D. Armstrong, J. G. Beery, and A. G. Blair, Phys. Rev. **182**, 1113 (1969).
[34]H. Iida, Y. Aoki, K. Hashimoto, M. Matoba, K. Nagano, H. Sakamoto, Y. Tagishi, M. Takei, H. Tanaka, and K. Yagi, in *Proceedings of the RCNP International Symposium on the Light Ion Reaction Mechanism, Osaka, 1983* (RCNP, Osaka University, 1983), p. 477.
[35]J. M. Lohr and W. Haeberli, Nucl. Phys. **A232**, 381 (1974).
[36]W. W. Daehnick, J. D. Childs, and Z. Vrcelj, Phys. Rev. C **21**, 2253 (1980).
[37]N. B. Gove and A. H. Wapstra, Nucl. Data Tables **11**, 127 (1972).
[38]G. R. Satchler, *Direct Nuclear Reactions* (Clarendon, Oxford, 1983).
[39]R. C. Johnson, Nucl. Phys. **35**, 654 (1962).
[40]A. Bohr, in *International Symposium on Nuclear Structure, Dubna, 1968* (International Atomic Energy Agency, Vienna, 1969), p. 179.
[41]D. R. Bes and R. A. Broglia, Nucl. Phys. **80**, 289 (1960).
[42]K. Sato, Ph. D. thesis, Osaka University, 1974.
[43]T. Udagawa, T. Tamura, and T. Izumoto, Phys. Lett. **35B**, 129 (1971).
[44]T. Yule and W. Haeberli, Phys. Rev. Lett. **19**, 756 (1967).
[45]W. T. Pinkston and G. R. Satchler, Nucl. Phys. **A383**, 61 (1982).
[46]M. Igarashi and K.-I. Kubo, in *Proceedings of RCNP International Symposium on the Light Ion Reaction Mechanism, Osaka, 1983* (RCNP, Osaka University, 1983), p. 376.
[47]*Table of Isotopes,* 7th ed., edited by C. M. Lederer and V. S. Shirley (Wiley, New York, 1978), pp. 362 and 712.
[48]This sign corresponds to the case in which the value $\langle \vec{L}\cdot\vec{\sigma} \rangle$ is positive.